

Identification and Control of Multirotor Actuator Dynamics with RPM feedback

Sesha Charla

September 24, 2023

Contents

I	Model Parameter Identification	3
1	Brushless DC motor model	3
1.1	Brushless DC motor speed-torque characteristics [1]	3
1.2	Dynamic Model (without Propeller)	4
1.3	BLDC Motor with Propeller	4
1.4	Propeller Aerodynamics	5
1.4.1	Parameter estimation from the static data	5
2	RPM Measurement	7
2.1	Measurement Algorithm	9
3	Input definition and Static Calibration	10
3.1	ESC and non-linear input compensation	10
3.2	Normalized Angular Velocity Input	10
4	BLDC Motor with Propeller Model – Parameter Estimation	12
4.1	Small Perturbation Model	12
4.1.1	Linearized Model Parameter Estimation	13
4.1.2	Validation using the response of the full non-linear model	13
II	Control	15
5	Control Model and Input	15
6	Adaptive Robust Control Designs	16
6.1	Direct Adaptive Robust Control Design (ARC)	16
6.2	Direct-Indirect Adaptive Robust Control Design (DIARC)	16
7	Disturbance Observer based Controller Designs	16
7.1	DOB Design	16
7.2	Active Disturbance Rejection Controller Design (ADRC)	16
8	Comparative Study	16
9	Conclusion	17

10 Appendix	18
10.1 Linearized Model Validation	18
10.1.1 Experiment Details	18
10.1.2 Frequency Domain Validation	18
10.1.3 Time Domain Validation	19

Part I

Model Parameter Identification

1 Brushless DC motor model

1.1 Brushless DC motor speed-torque characteristics [1]

The torque and speed characteristics can be determined by the balance between motor's mechanical output power and electrical input power over a conduction period:

$$P = \omega_m T_e = 2e_p I$$

$$e_p = N_p B_g \pi r l \omega_m$$

Where,

ω_m – Mechanical rpm

T_e – Electromagnetic torque

e_p – Back emf

The factor 2 is the result of current flowing through 2-motor phases (trapezoidal wave form).

We have, electromagnetic torque:

$$T_e = 4N_p B_g l r I \quad [\because \text{Lenz law}]$$

let, $E = 2e_p$. We have,

$$E = k\psi\omega_m = K_v\omega_m$$

$$T_e = k\psi I = K_T I$$

Where,

$$k = 4N_p \quad (\text{Armature Constant})$$

$$\psi = B_g \pi r l \quad (\text{Flux})$$

Thus, ideally back-emf constant and torque constants are same.

Using the above equations, the following steady-state torque speed characteristics can be derived. We have, the instantaneous voltage equation:

$$V_s = E + IR$$

Where,

V_s – Supply voltage

I – Total DC current

R – Sum of the terminal phase resistances

We have torque speed relationship:

$$\omega_m = \omega_0 \left(1 - \frac{T}{T_0} \right)$$

Where,

$$\omega_0 = \frac{V_s}{k\psi} \quad (\text{No-load Speed})$$

$$T_0 = k\psi I_0 \quad (\text{Stall Torque})$$

$$I_0 = \frac{V_s}{R} \quad (\text{Stall Current})$$

1.2 Dynamic Model (without Propeller)

We have the dynamic model of BLDC motor using moment balance:

$$J_m \dot{\omega}_m = T_e - b_f \omega_m - M_f$$

where,

J_m – Moment of inertia of the motor

b_f – lumped parameter for viscous friction

M_f – lumped parameter for coulomb friction

Friction:

1. Viscous friction: $-b_f \omega$.
2. Columb friction: $-M_f \text{sign}(\omega) = -M_f$ [\because the motor turns in only one direction].

From the speed-torque characteristics of the BLDC motor:

$$T_e = K_T I = K_T \frac{(V_s - E)}{R} = \frac{K_T}{R} (V_s - K_v \omega_m) \quad [\because K_v = K_T = k\psi]$$

Let,

$$K_r = \frac{K_T}{R}$$

From the definition of Input to ESC:

$$\begin{aligned} V_s &= u V_{in} \\ \therefore T_e &= u K_r V_{in} - K_r K_v \omega_m \end{aligned}$$

Substituting:

$$\begin{aligned} J_m \dot{\omega}_m &= u K_r V_{in} - K_r K_v \omega_m - b_f \omega_m - M_f \\ b_m &= K_r K_v + b_f \end{aligned} \quad \text{Let}$$

$$\boxed{J_m \dot{\omega}_m + b_m \omega_m + M_f = u K_r V_{in}} \quad (1)$$

1.3 BLDC Motor with Propeller

Adding propeller moment of inertia and the moment due to propeller drag into the BLDC motor model.

$$(J_m + J_p) \dot{\omega} + b_m \omega + M_f = u K_r V_{in} - C_D \omega^2$$

Where, C_D is the aerodynamic drag. Let, $J_m + J_p = J$

$$\boxed{J \dot{\omega} + b_m \omega + C_D \omega^2 + M_f = u K_r V_{in}} \quad (2)$$

1.4 Propeller Aerodynamics

Aerodynamics are assumed to be faster than mechanical dynamics of the actuator. The thrust generation process due to the propagation of pressure wave is assumed to be instantaneous. This assumption is inherent to the standard models that use potential flow theory (lifting-line, blade-element and momentum-disk theories), as they assume incompressible flow.

Propeller Thrust:

$$F_T = C_T \omega^2$$

Propeller moment due to drag:

$$M_D = C_D \omega^2$$

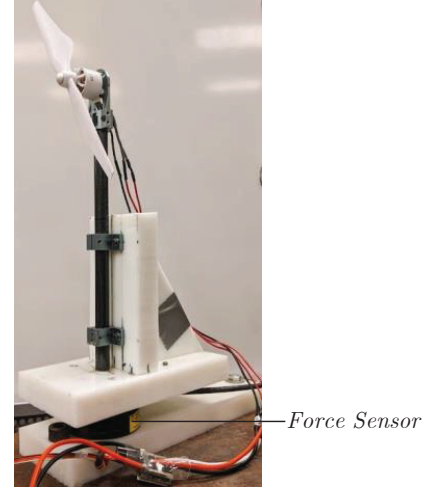


Figure 1: Experimental Setup

Aeroelasticity of the propeller: It is assumed that the aeroelasticity of the propeller produces high-frequency oscillations in the thrust and torque of the propeller which are assumed to be very fast and roll off w.r.t the mechanical dynamics of the actuator as well as the transmission through the propeller shaft. The constant bias in the torque due to flutter is captured in the drag coefficient and its parameter uncertainty.

1.4.1 Parameter estimation from the static data

In the experimental setup (Figure 1), the total moment measured is the result of aerodynamic moment and the friction of the BLDC motor. Thus the total moment becomes:

$$M = C_D \omega^2 + b_f \omega + M_f$$

The aerodynamic coefficients are estimated from the static measurements using least-squares estimation.

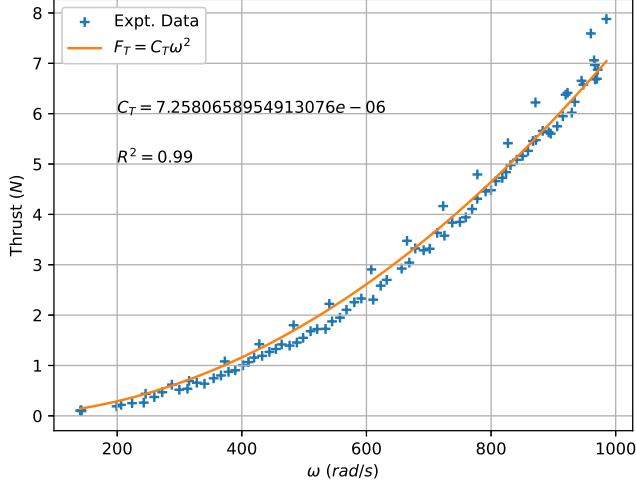


Figure 2: Variation of thrust with rpm

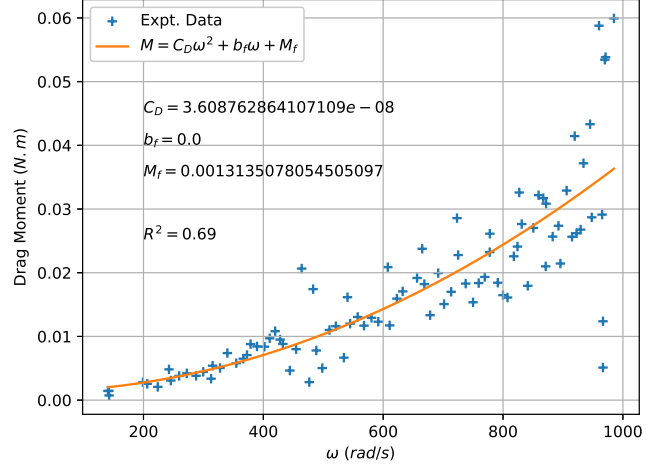


Figure 3: Variation of drag moment with rpm

The moment data has more variation from model due to the unmodelled aerodynamic effects such as aerodynamic-flutter. Thus we have the estimates of force coefficients:

Parameter	Value
C_T	$7.2581 \times 10^{-06} \text{ N}/(\text{rad}/\text{s})^2$
C_D	$3.6088 \times 10^{-08} \text{ N.m}/(\text{rad}/\text{s})^2$
b_f	$0.0 \text{ N.m}/(\text{rad}/\text{s})$
M_f	$1.3135 \times 10^{-3} \text{ N.m}$

Table 1: Estimates Force coefficients

2 RPM Measurement

An interrupt is triggered for every commutation high and the ISR gets the counter value of an independently running timer. Using this value, the RPM is calculated at every interrupt trigger as follows:

$$rpm = \frac{60 f_t}{N_p \times T_c}$$

Where,

f_t – Frequency of the timer counts (here, 1 MHz)

N_p – Number of pole-pairs in the BLDC motor (here, 7)

T_c – Timer counts between the two interrupts

The above method of measurement is verified against the tach-meter reading. The readings are in agreement with each other, validating the measurement method.

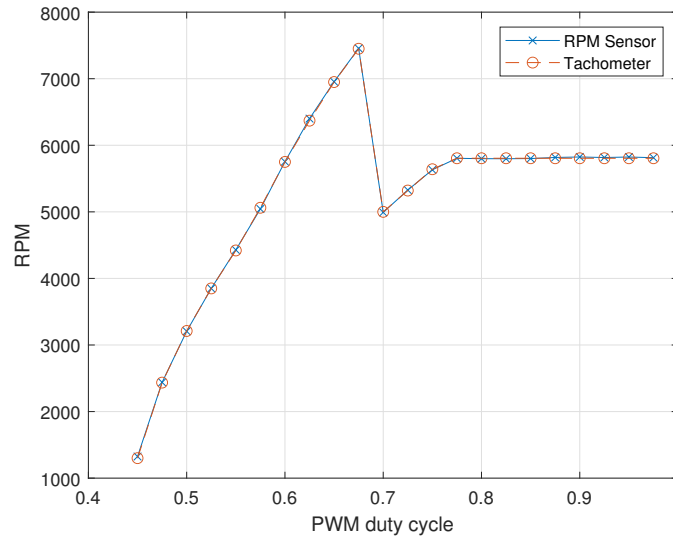


Figure 4: Rpm sensor and tachometer readings

The above method has an inherent flaw at very low *rpms* where there is no commutation at a given sampling instance which results in a zero rpm at that sample making the sensor noisy. This can be avoided by holding the rpm value from the previous measurement if there is no commutation in the sample instance.

Using external interrupt and timer

The commutations can be counted using external interrupts. The actual measurement of rpm involves a raising-edge triggered external interrupt and a timer interrupt. The ISR of the external interrupt updates a counter corresponding to the pulses (here, the electrical commutations). The timer-interrupt polls for this counter value at the specified frequency (f_s) and resets the counter. The rpm is calculated from this counter value as follows:

$$rpm = \frac{counter_value}{N_p} \times f_s \times 60$$

where,

N_p – No. poles in the BLDC motor

The minimum rpm that can be measured depends on the sampling frequency and the poles in the BLDC motor ($= \frac{60f_s}{N_P}$). And the maximum depends on the clock frequency of the micro-controller as the frequency of interrupts and ISR calls becomes the bottleneck in this case. The resolution of the sensor also depends on the sampling frequency and poles as the counter value is an integer. We have,

$$Sensor\ resolution = \frac{60f_s}{N_P}$$

For the current system the range of rpm is [2000, 10000]. The number of poles in BLDC motor are 12. Assuming the acquisition frequency of 400 Hz, the resolution for the above sensor will be:

$$Sensor\ resolution = \frac{60f_s}{N_P} = 2000\ rpm = 209.4395\ rad/s$$

For 100 Hz acquisition rate:

$$Sensor\ resolution = 500\ rpm = 52.3599\ rad/s$$

The main source of sensor noise in this case is the latency of the external interrupt. The counter value will be oscillating around the actual value based on the timing of external and timer interrupts causing the measured rpm to fluctuate. Based on the resolution calculations above, the signal-to-noise ratio of the system will be very high if the current implementation is used.

This problem of resolution and signal-to-noise ratio is due to the interfacing method used. Alternatively, the following method is proposed to overcome this problem.

Using two timers and an external interrupt

We use an additional timer as a high frequency counter of frequency f_t for calculating the rpm at every sampling period as follows:

$$rpm = \frac{counter_value \times f_t}{N_P \times time_counts} \times 60$$

where,

N_P — No. poles in the BLDC motor

$time_counts$ — Number of timer interrupt counts during the sampling interval.

Hence, we have, maximum number of $time_counts$ in a sampling interval is f_s/f_t

$$\implies Sensor\ resolution = \frac{60f_s}{N_P f_t} = rpm_{min}$$

Therefore, the resolution of the sensor can be increased by arbitrarily increasing the frequency of the high frequency counter, limited only by the hardware.

For example, if $f_h = 1000\ Hz$, for the same values as above, the resolution of the sensor:

$$Sensor\ resolution = \frac{60f_s}{N_P \times f_t} = \frac{2000}{1000} = 2\ rpm = \frac{1}{\pi}\ rad/s$$

This method will reduce the signal-to-noise ratio significantly.

2.1 Measurement Algorithm

In higher rpm cases there are more than one measurement instance within the sample time. Median of these measurements can be used to reduce sudden spikes in the data due to interrupts skips. Combining this with higher resolution algorithm, we have the algorithm for rpm measurement:

Let C_c be the current value of the 32-bit timer, P_c the previous value and n_C be the number of computations within the sample.

At every interrupt trigger (in ISR)

```

 $n_C += 1;$ 
 $\delta t_k = C_c - P_c;$ 
if  $\delta t_k \leq 0$  then
    |  $\delta t_k += 2^{32};$                                 /* Correcting for integer overflow */
end
 $\delta t_k[n_C - 1] = \delta t_k;$ 
 $P_c = C_c;$ 

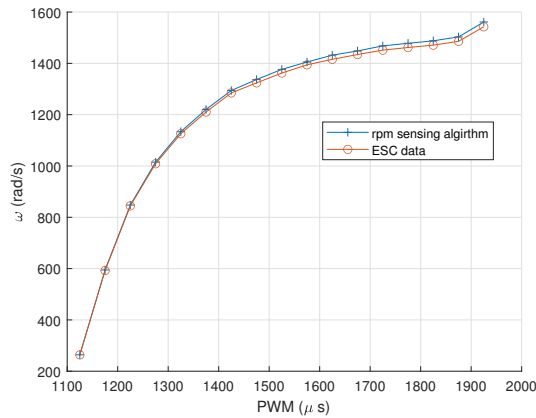
```

At every sampling instance (in *get_rpm()*):

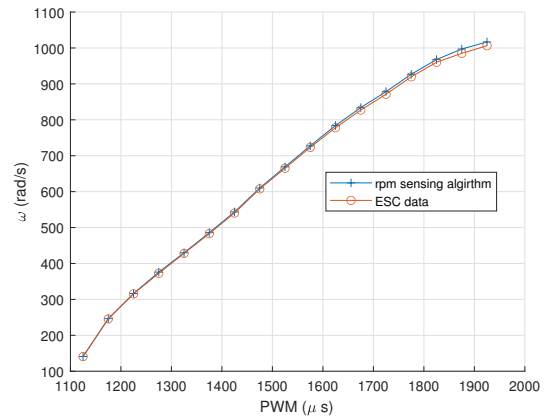
```

 $N_p = 7;$ 
 $f_t = 10^6;$ 
 $M = \frac{2\pi}{N_p} \times f_t;$ 
if  $n_C > 0$  and  $n_C \leq n_{C_{max}}$  and  $|n_C - n_{C_{old}}| \leq \delta n_{C_{max}}$  then
    |  $\omega = \frac{M}{\text{Median}(\delta t_k)};$                                 /* Median removes spikes in the data */
    |  $\omega_{old} = \omega;$ 
    |  $n_{C_{old}} = n_C;$ 
else
    |  $\omega = \omega_{old}$ 
end
 $n_C = 0;$ 
 $\delta t_k = 0;$ 

```



Without Propeller



With Propeller

Figure 5: Validating the measurement algorithm

3 Input definition and Static Calibration

3.1 ESC and non-linear input compensation

The castle creations ESC has a micro-controller that non-linearly scales the input PWM signal's duty-cycle to the duty-cycle of the 24 kHz —PWM signals to the inverter effectively scaling the source voltage to the motor by the duty-cycle. This is done to have a linear input to thrust curve instead of a quadratic one.

The input transmission can be described as follows: The 400 Hz —PWM duty cycle (u_p) is linearly scaled to a throttle ratio (p) (% power-out) between 0 and 1. Which is then filters using a non-linear function (g_u) to get the PWM duty-cycle input to the inverter (u) [2].

$$u_p \rightarrow \boxed{g_u(\cdot)} \rightarrow u$$

and finally,

$$V_s = uV_{in} \quad u \in [0, 1]$$

u is considered as the input to the motor-propeller system and the necessary inversion will be performed for transmitting the signals.

Scaling PWM Singal Duty cycle based on switching frequency: Pixhawk-4 uses a switching frequency of 400 Hz for its PWM signals (can be swithed to 50 Hz which is not that usefull in case of BLDC motors but usefull for servos). The controller thus scales the PWM duty cycle to the duration of on-time of the signal in its period in 'microseconds'. These inputs are handelled as integer types within the range $[800, 2200]$ [3].

The current ESC that has the rpm-feedback capabilites has an operating range between $1110\text{ }\mu\text{s}$ and $1890\text{ }\mu\text{s}$. After that, the ESC switches to a constant power mode which sets the rpm to a constant.

$$\begin{aligned} \text{Period of the PWM wave} &= \frac{1}{400} \times 10^6 \text{ }\mu\text{s} = 2500 \text{ }\mu\text{s} \\ \text{Minimum Operating Duty Cycle} &= \frac{1110}{2500} = 0.444 \\ \text{Maximum Operating Duty Cycle} &= \frac{1890}{2500} = 0.756 \end{aligned}$$

u can be considered to be the actual input to the system and system identification with the propeller. It turns out that the parameters of the above non-linear filter are not estimatable with the give information. To solve this problem, we chose angular velocity of the motor with propeller normalized with voltage as the input instead.

3.2 Normalized Angular Velocity Input

We have the no-load dynamic model for the BLDC motor with propeller:

$$J\dot{\omega} + b_m\omega + C_D\omega^2 + M_f = uK_rV_{in}$$

At steady state ($\dot{\omega} = 0$), the above equation becomes:

$$\begin{aligned} b_m\omega + C_D\omega^2 + M_f &= uK_rV_{in} \\ \Rightarrow \frac{b_m}{K_r} \left(\frac{\omega_m}{V_{in}} \right) + \frac{V_{in}}{K_r} C_D \left(\frac{\omega}{V_{in}} \right)^2 + \frac{M_f}{K_rV_{in}} &= u \end{aligned}$$

Definition: Let, u_ω be the angular velocity of the motor with propeller at unit supply voltage for the given pwm input (u_p). Also, let us call it ”**Normalized angular velocity**”.

$$u_\omega = \frac{\omega}{V_{in}} \text{ at } u = g_u(u_p)$$

$$\Rightarrow u = \underbrace{\frac{b_m}{K_r} u_\omega + \frac{\hat{V}_{in}}{K_r} C_D u_\omega^2 + \frac{M_f}{K_r \hat{V}_{in}}}_{g_\omega(u_\omega, \hat{V}_{in})}$$

The relationship between u_ω and u_p can be estimated from the staic measuremnt data.

We have:

$$u_\omega = a u_p + b \quad a = 0.0696 \quad b = -64.3266$$

Also,

$$\because u = g_\omega(u_\omega, \hat{V}_{in})$$

$$\Rightarrow g_u(u_p) = g_\omega(a u_p + b, \hat{V}_{in})$$

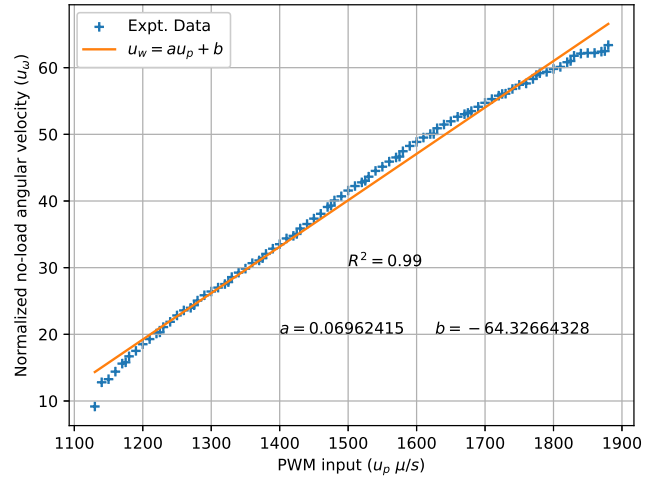


Figure 6: u_ω as a function of u_p

4 BLDC Motor with Propeller Model – Parameter Estimation

Introducing the input definition into the BLDC-motor model with propeller:

$$\begin{aligned}
 J\dot{\omega} + b_m\omega + C_D\omega^2 + M_f &= uK_rV_{in} = K_rV_{in}g_\omega(u_\omega, \hat{V}_{in}) \\
 \implies J\dot{\omega} + b_m\omega + C_D\omega^2 + M_f &= K_rV_{in} \left(\frac{b_m}{K_r}u_\omega + \frac{\hat{V}_{in}}{K_r}C_Du_\omega^2 + \frac{M_f}{K_r\hat{V}_{in}} \right) \\
 J\dot{\omega} + b_m\omega + C_D\omega^2 + M_f \left(1 - \frac{V_{in}}{\hat{V}_{in}} \right) &= V_{in}b_mu_\omega + V_{in}\hat{V}_{in}C_Du_\omega^2
 \end{aligned}$$

Note on Voltage: The battery voltage is assumed to be constant with small variations that can be introduced as uncertainties.

$$\begin{aligned}
 \hat{V}_{in} = V_{in}(1 + \delta v) &\implies \frac{V_{in}}{\hat{V}_{in}} = 1 - \delta v \implies \left(1 - \frac{V_{in}}{\hat{V}_{in}} \right) = \delta v \\
 J\dot{\omega} + b_m\omega + C_D\omega^2 + M_f\delta v &= V_{in}b_mu_\omega + V_{in}^2(1 + \delta v)C_Du_\omega^2
 \end{aligned} \tag{3}$$

4.1 Small Perturbation Model

We get the linearised model using small perturbation and neglecting the gain variation (δv):

$$\begin{aligned}
 J\delta\dot{\omega} + b_m\delta\omega + 2C_D\omega_0\delta\omega &= \delta u_\omega (V_{in}b_m + 2V_{in}^2C_Du_{\omega_0}) \\
 J\delta\dot{\omega} + (b_m + 2C_D\omega_0)\delta\omega &= \delta u_\omega (V_{in}b_m + 2V_{in}^2C_Du_{\omega_0}) \\
 \text{Laplace Transform:} \\
 (Js + (b_m + 2C_D\omega_0))\delta\omega &= \delta u_\omega (V_{in}b_m + 2V_{in}^2C_Du_{\omega_0})
 \end{aligned}$$

Thus we have the transnsfer function model:

$$\frac{\delta\omega(s)}{\delta u_\omega(s)} = \frac{V_{in}b_m + 2V_{in}^2C_Du_{\omega_0}}{Js + (b_m + 2C_D\omega_0)}$$

Also, we have the following relationship between the nominal input and outputs from the input-definition:

$$\begin{aligned}
 \omega_0 &= V_{in}u_{\omega_0} \\
 \implies \frac{\delta\omega(s)}{\delta u_\omega(s)} &= \frac{V_{in}(b_m + 2C_DV_{in}u_{\omega_0})}{Js + (b_m + 2C_D\omega_0)} = \frac{V_{in}(b_m + 2C_D\omega_0)}{Js + (b_m + 2C_D\omega_0)} \\
 &= \frac{V_{in}}{\left(\frac{J}{b_m + 2C_D\omega_0} \right) s + 1} \quad \left(= \frac{K_m}{\tau_ms + 1} \right) \\
 \implies K_m &= V_{in} \\
 \tau_m &= \frac{J}{b_m + 2C_D\omega_0} \\
 \implies \omega_m &= \frac{1}{J} (b_m + 2C_D\omega_0)
 \end{aligned}$$

Thus time-constant decreases with the nominal rpm and the static gain is purely a function on the battery voltage.

This information will be used for establishing the validity of identified model. Sum-of-Sinusoids input is used around a nominal input for generating the frequency response of the system to identify the model.

In case of using u_p as input:

$$\begin{aligned}
u_\omega &= au_p + b \\
\Rightarrow \delta u_\omega &= a\delta u_p \\
\Rightarrow \frac{\delta \omega(s)}{\delta u_p(s)} &= \left(\frac{1}{a}\right) \frac{K_m}{\tau_m s + 1}
\end{aligned}$$

Thus this results in variation of the static gain alone.

4.1.1 Linearized Model Parameter Estimation

The response of the system to Sum-of-Sinusoids signal at 250 Hz and $50\mu s$ (PWM) amplitude containing 299 frequencies in the range $[0.01, 30]\text{ Hz}$ is used for first-order model parameter identification. The nominal inputs and the corresponding rpm is tabulated in Table 3. The identified models are validated against the response of a chirp signal with the same frequency range and sampling frequency. The validation results are plotted in Section 10.1.

The estimates static-gain and cut-off frequencies are plotted with nominal inputs. The corresponding parameters relating them to the nominal inputs are estimated using least-squares method.

The V_{in} and K plot demonstrates the validity of their relationship when the V_{in} variation is included, i.e.,

$$K = V_{in}(1 + \delta v)$$

The variation of cut-off frequency with nominal rpm gives the estimates of propeller moment of inertia and the damping as follows:

$$\begin{aligned}
J &= 3.2238 \times 10^{-6} \text{ Kg.m}^2 \\
b_m &= 0
\end{aligned}$$

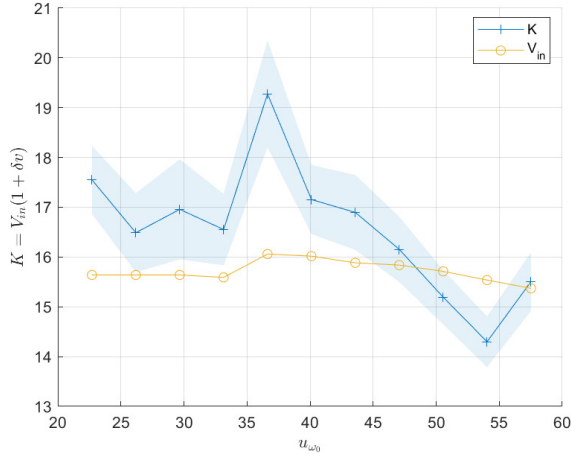


Figure 7: Static gain and Voltage input

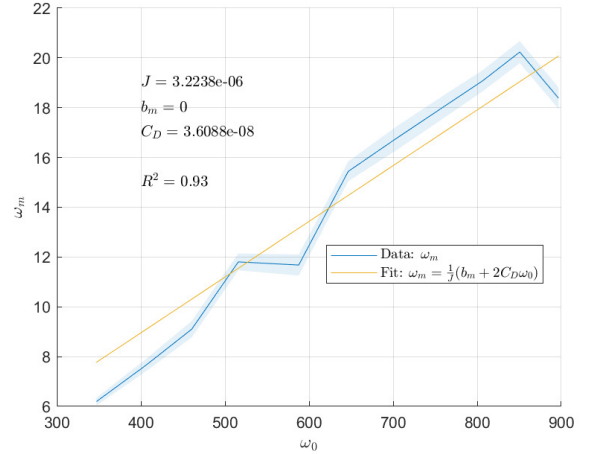


Figure 8: Cut-off frequency

4.1.2 Validation using the response of the full non-linear model

We have the model parameters identified:

Parameter	Value	
C_T	7.2581×10^{-06}	$N/(rad/s)^2$
C_D	3.6088×10^{-08}	$N.m/(rad/s)^2$
b_m	0.0	$N.m/(rad/s)$
M_f	1.3135×10^{-3}	$N.m$
J	3.2238×10^{-6}	$Kg.m^2$

Table 2: Summary of parameter estimates from static and small-perturbation experiments

Assuming $\delta v = 0$ we have the non-linear model of the system eqn 3:

$$J\dot{\omega} + b_m\omega + C_D\omega^2 = V_{in}b_mu_\omega + V_{in}^2C_Du_\omega^2$$

The above model is simulated with the identified parameters using a square wave and chirp input whose amplitude covers the full operating range. The results of the simulation are then compared with the experimental data.

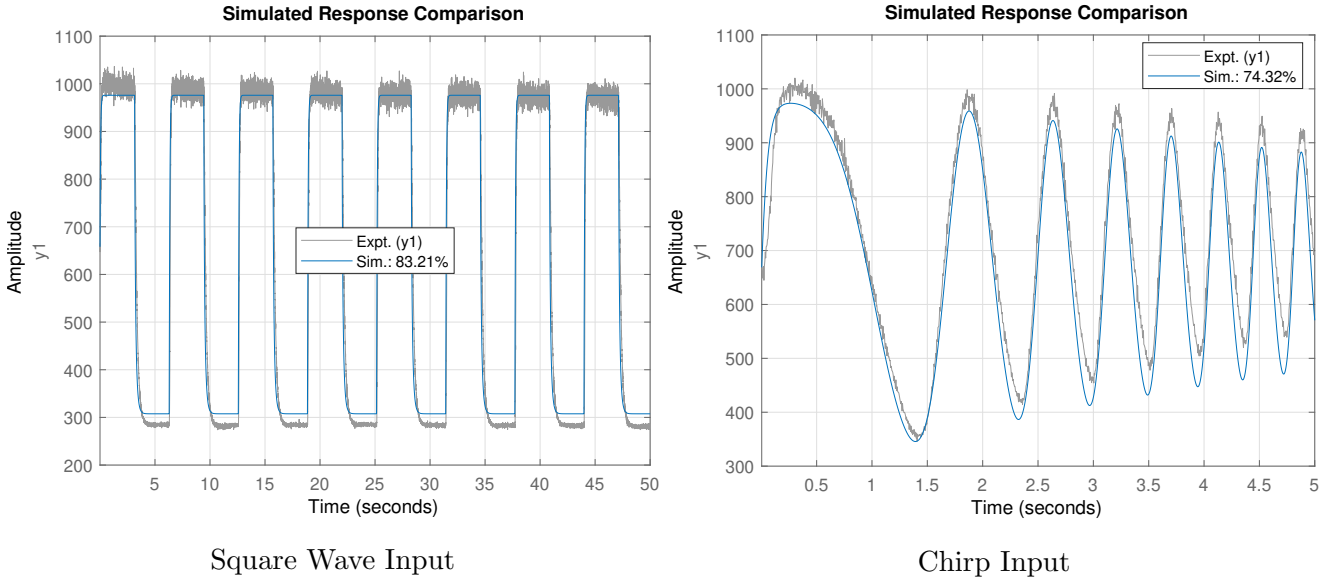


Figure 9: Model Validation

Form the Figure 9, it can be concluded that the model parameters are estimated with a reasonable accuracy. The error in simulation as compared to the esperiment can be primarily attributed to theh δv that needs to me estimated in real-time.

Part II

Control

5 Control Model and Input

From parameter estimates (Table 2), it can be seen that the estimate of total 'damping' factor (b_m) is zero. Thus, the linear term of the control input in the RHS of eqn. 3 can be ignored. Let $u = u_\omega^2$ be the control input to the system for which we are going to design the feedback controller. Incorporating the above two assumptions into eqn. 3, we have the control form of the model:

$$J\dot{\omega} + b_m\omega + C_D\omega^2 + M_f\delta v = V_{in}^2(1 + \delta v)C_D u \quad (4)$$

We have the following bounds on the control input:

$$\begin{aligned} u &= u_\omega^2 = (au_p + b)^2 \\ \Rightarrow u_{min} &= (au_{p_{min}} + b)^2 = (0.0696 \times 1110 - 64.3266)^2 = 167.1694 \\ \Rightarrow u_{max} &= (au_{p_{max}} + b)^2 = (0.0696 \times 1890 - 64.3266)^2 = 4518.1789 \end{aligned}$$

The goal of feedback control design for the actuator is two-fold:

1. Compensate for the input-uncertainties, un-modelled disturbances and model-structure errors.
2. Make the actuator track the response of a second-order transfer function with no over-shoot of the form:

$$G_{ref}(s) = \frac{1}{s^2 + 2\zeta\omega_{ref} + \omega_{ref}^2} \quad \zeta = \frac{1}{\sqrt{2}} = 0.707$$

Such that, ω_{ref} results in the maximum possible bandwidth in presence of uncertainties mentioned above.

To this end, two feedback control design theories are used:

1. Adaptive robust control (ARC) theory based designs:
 - (a) Direct/Indirect Adaptive Robust Controller (DIARC).
 - (b) ARC design with parameter estimation only for the disturbances (Disturbance ARC) for comparing with the classical DOB design.
2. Disturbance Observer (DOB) base designs:
 - (a) Classical DOB design.
 - (b) Active Disturbance Rejection Controller (ADRC).

6 Adaptive Robust Control Designs

6.1 Direct Adaptive Robust Control Design (ARC)

6.2 Direct-Indirect Adaptive Robust Control Design (DIARC)

7 Disturbance Observer based Controller Designs

7.1 DOB Design

7.2 Active Disturbance Rejection Controller Design (ADRC)

8 Comparative Study

9 Conclusion

10 Appendix

10.1 Linearized Model Validation

10.1.1 Experiment Details

Expt.	u_{p0} (μs)	u_{ω_0} ($rad/(s.V)$)	ω_0 (rad/s)
1	1250	22.7035	347.1147
2	1300	26.1848	405.6932
3	1350	29.6660	460.4567
4	1400	33.1472	515.9106
5	1450	36.6284	587.6871
6	1500	40.1096	646.5961
7	1550	43.5908	703.7016
8	1600	47.0720	756.4896
9	1650	50.5532	806.9497
10	1700	54.0344	850.6007
11	1750	57.5156	896.7785

Table 3: Nominal Inputs

$$f_s = 250 \text{ Hz}$$

[Sampling Frequency]

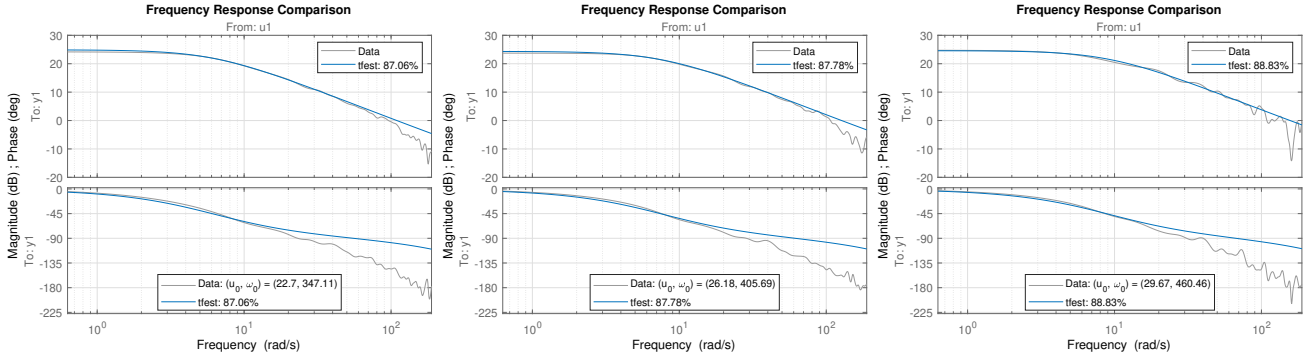
$$t_f = 50 \text{ s}$$

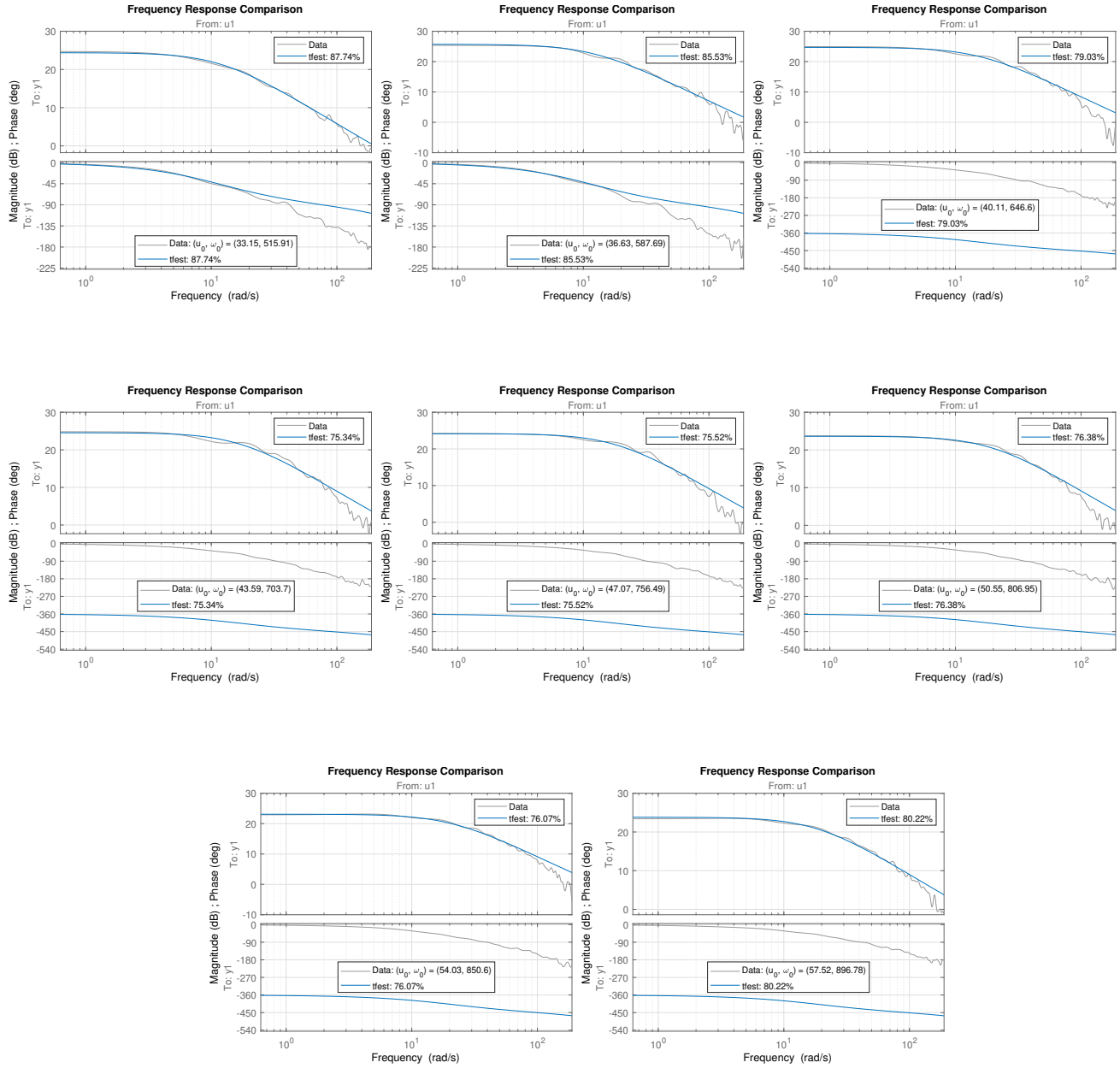
[Final Time]

$$N_p = 10$$

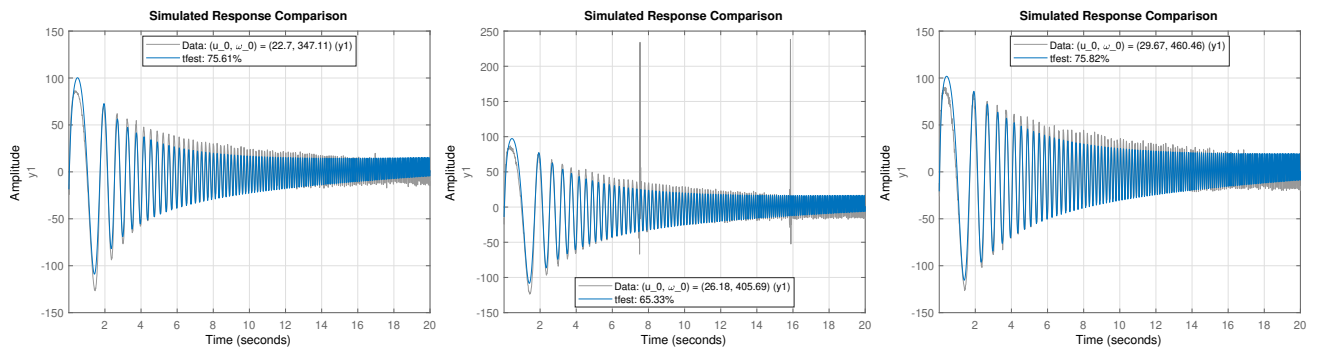
[Number of Periods]

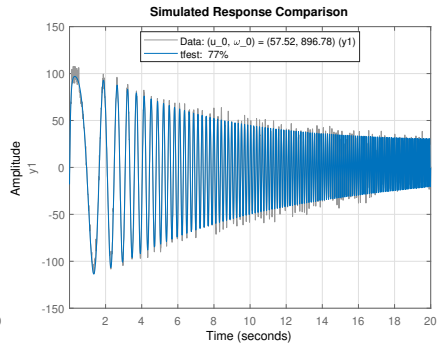
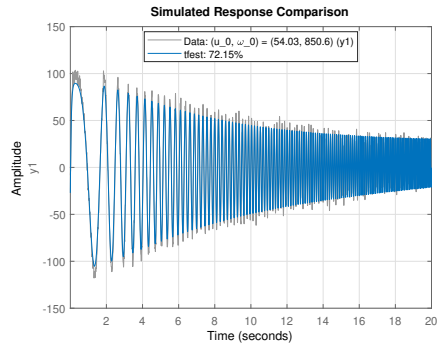
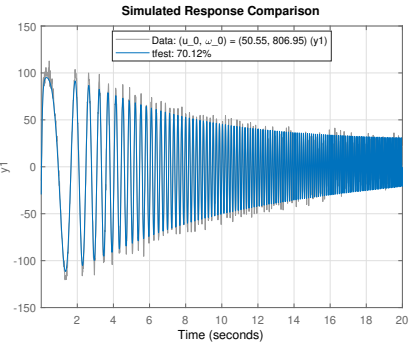
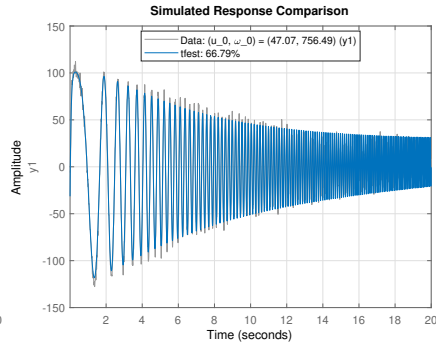
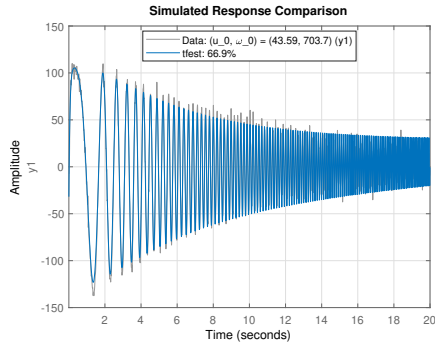
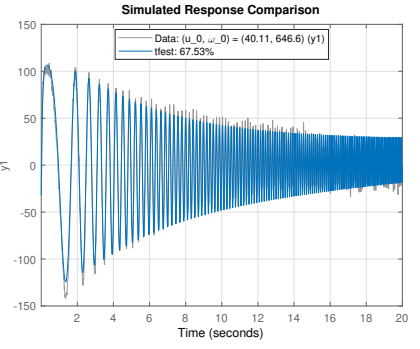
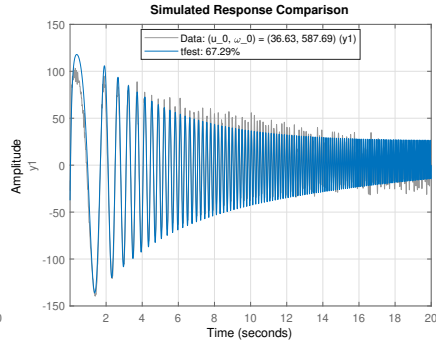
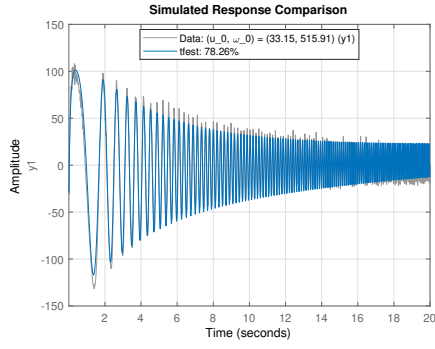
10.1.2 Frequency Domain Validation





10.1.3 Time Domain Validation





References

- [1] Richard Crowder. *Electric drives and electromechanical systems: applications and control*. Butterworth-Heinemann, 2019.
- [2] Sang-Hoon Kim. *Electric motor control: DC, AC, and BLDC motors*. Elsevier, 2017.
- [3] Pixhawk-4 user manual. https://docs.px4.io/main/en/peripherals_pwm_escs_and_servo.html#pwm-servos-and-escs-motor-controllers.